BIOMARKERS, 2000, VOL. 5, NO. 1, 56–72

An NMR-based metabonomic investigation of the toxic effects of 3-trifluoromethyl-aniline on the earthworm *Eisenia veneta*

MARK A. WARNE[1], E. M. LENZ[1], D. OSBORN[2], J. M. WEEKS[2] and J. K. NICHOLSON[1]*

[1] Biological Chemistry, Biomedical Sciences Division, Imperial College of Science, Technology and Medicine, Sir Alexander Fleming Building, London SW7 2AZ, UK.

[2] Institute of Terrestrial Ecology, Monks Wood, Abbots Ripton, Huntingdon, Cambridgeshire, PE17 2LS, UK

Received 1 March 1999, revised form accepted 21 June 1999

^{1}H NMR spectra of earthworms *Eisenia veneta* treated with 3-trifluoromethyl-aniline in a 72-h contact filter paper test have been analysed using pattern recognition techniques to determine the biochemical response. Various strategies for data reduction of the metabolite profile, and illustration by principal components analysis are applied and discussed. The use of mean principal components plots in simplifying group data representation and highlighting the dose–response function is demonstrated. Hierarchical cluster analysis, and cluster significance analysis of the principal components were also used to examine the relative distribution of dose groups. Identification and assignment of metabolite responses to toxicity were found via correlation coefficient-shift plots. As measured by the correlation coefficients alanine was the most significant metabolite, but increased levels of other amino acids such as glycine and asparagine were also observed. Further, elevated levels of glucose, and the citric acid cycle intermediates citrate and succinate were noted as potential biomarkers of toxicity. This work provides a basis for examining the biochemical response of invertebrates to toxins. This should provide a framework to examine toxicity effects of other halogenated aromatic pollutants to earthworms used as environmental monitors.

Keywords: trifluoromethyl-aniline, NMR, pattern recognition, earthworm, *Eisenia veneta*.

Biomarkers Downloaded from informahealthcare.com by Changhua Christian Hospital on 11/18/12
For personal use only.

Introduction

There is strong current demand for novel biochemical biomarkers of exposure and effect in species that are open to contamination by environmental chemicals. One of our long-term aims is to understand the molecular toxicology of halo-aromatic compounds in invertebrate species. Hence, we are involved in the development of new methods for understanding mechanistic toxicological responses and for novel biomarker generation in species with pollution indicator potential. There is also considerable interest in novel biomarker and surrogate marker information in the pharmaceutical industry, and a series of new technologies are being developed with this aim in mind. The most widely known new approaches involve measurements of responses of living systems to xenobiotics at the genetic level (genomics) and at the level of expression of cellular proteins (proteomics). Both of these approaches are potentially very powerful, both for drugs and environmental chemicals, and offer different levels of understanding the response to xenobiotic exposure, yet both are incomplete with respect to

* To whom correspondence should be addressed; e-mail: j.nicholson@ic.ac.uk

Biomarkers ISSN 1354-750X print/ISSN 1366-5804 online © 2000 Taylor & Francis Ltd
http://www.tandf.co.uk/journals/tf/1354750X.html

RIGHTSLINK

providing information and understanding of integrated cellular function and the development of post-exposure dysfunction with time. Thus we have proposed a concept which provides complementary toxicological and novel biochemical biomarker information. This concept is termed 'metabonomics', which we define simply as 'the quantitative measurement of the time-related multiparametric metabolic response of living systems to pathophysiological processes' (Holmes *et al.* in press). The approach has arisen both from our work in metabolic ^{1}H NMR spectroscopy of cells, tissues and biofluids (Nicholson and Wilson 1989) and more particularly in our more recent work utilizing pattern recognition, expert systems and other bioinformatic tools to interpret these complex NMR-generated metabolic data sets (see Nicholson *et al.* 1985, Nicholson and Wilson 1989, Gartland *et al.* 1991, Anthony *et al.* 1994, Beckwith-Hall *et al.* 1998 and Holmes *et al.* 1998 for examples). In the present work we have applied and evaluated the NMR-based metabonomic approach to an invertebrate system with a representative halo-aromatic compound, namely 3-trifluoromethyl-aniline (TFMA).

The advantages of the use of pattern recognition (PR) methods to analyse the biological ^{1}H NMR spectra become apparent when the nature of the spectra are considered. ^{1}H NMR spectroscopy offers an efficient means of non-destructively detecting and quantifying low molecular weight compounds in small samples. The basic NMR spectrum non-selectively displays all these metabolites from the biofluid or tissue extract as a line plot differentiated by chemical shift on the x-axis. The chemical shift of the metabolite is dependent upon the chemical environment of the proton of the metabolite, with several signals possible for metabolites with several protons. The relative amount of the metabolite present can be found from the area of the signal, with the intensity as the y-axis. Thus each spectrum can contain perhaps hundreds of signals of varying intensity. To analyse unknown and often subtle changes between a series of spectra is only feasible using PR techniques.

Whereas ^{1}H NMR and PR (metabonomic) methods have proved useful in detecting potential biomarkers in mammalian species, little NMR work has been performed on invertebrate species. We have previously used the NMR-PR approach to identify histidine as a novel biomarker of copper toxicity to *Eisenia andrei* and *Lumbricus rubellus* (Gibb *et al.* 1997a). This approach was also applied to the assignment and comparison of six invertebrate species (Gibb *et al.* 1997b), including the two mentioned earthworms, identifying 30 metabolites. The inter-species variations were examined by principal components analysis (PCA) and hierarchical cluster analysis (HCA) of the identified metabolites.

However, the use of the general NMR-based metabonomic approach to the toxicity of organic pollutants to earthworms is both novel and as yet undeveloped, and may be of considerable importance in future environmental science, as well as in the pharmaceutical industry. The aim of the current work was to examine the metabolite profile of untreated and dosed earthworms, using standard environmental test conditions. The experimental conditions themselves are often designed with other criteria in mind, and may not be optimal for ^{1}H NMR spectroscopic studies. The optimization of the PR approach to detecting subtle differences between untreated and treated earthworms, *Eisenia veneta*, with TFMA was examined here. This compound will act as a test of this general approach to determine the toxicity of the class of halogenated aromatic pollutants, such as halo-

Biomarkers Downloaded from informahealthcare.com by Changhua Christian Hospital on 11/18/12
For personal use only.

RIGHTSLINK

Table 1. Dosing concentrations of TFMA and their physical effect on *Eisenia veneta*.

Dose group	Effective initial concentration (mg cm^{-2})	Physical effect
Dose 1	1.0	10 worms instantly died
Dose 2	0.1	9 worms instantly died 1 worm died (< 24 h)
Dose 3	0.01	No effect
Dose 4	0.001	No effect
Dose 5	0.0001	No effect
Control	None	No effect

benzenes, phenols, anilines and toluenes. However, this should also provide a basis for future work on the toxicology of a variety of organic pollutants in invertebrates.

Due to the complexity of the spectra the use of automatic data reduction prior to multivariate analysis is helpful. This was achieved by reducing the spectra into integrated regions of equal spectral width followed by PCA. PCA allows both a reduction in the dimensionality of the problem with consideration to the overall variance in the data, and also simplified data visualization (Livingstone 1995). This work will concentrate upon this technique, with emphasis on the visualization of the statistics wherever possible.

The toxicity of five chloroanilines (3-chloro-, 2,4-dichloro-, 2,4,5-trichloro-, 2,3,5,6-tetrachloro- and pentachloro-anilines) to the earthworms *Eisenia andrei* and *Lumbricus rubellus* in soil systems have been investigated by van Gestel and Ma (1990, 1993), van Gestel *et al.* (1991). The only reported toxicology end-point was the LC_{50} values. In preliminary work van Gestel (1991) also reported the soil and filter paper LC_{50} for 3,4-dichloroaniline. A more comprehensive filter paper study of a series of chloroanilines to *E. foetida* by Payaperez *et al.* (1995) found the LC_{50} toxicity to increase by a factor of two with increasing number of chlorines, but showed little effect with the chlorine substitution pattern. Payaperez and Mannone (1997) also reported soil toxicity of *E. foetida* to 2,4,5-trichloro- and 2,3,5,6-tetrachloro-aniline. However, in all these studies the biochemical effect of the haloanilines on endogenous metabolites of the earthworm was not investigated. This will be the main subject of this paper.

Materials and methods

Compound dosing and sample preparation

The standard filter paper contact toxicity test was conducted following the OECD guidelines (1984), whereby all the worms were allowed to depurate for 24 h prior to the commencement of the dosing.

The filter paper was prepared to a total area of 50.4 cm^2. A standard solution of TFMA (393 µl/9607 µl TFMA/hexane, i.e. 0.03 M TFMA stock) was diluted (1/10) to match the required exposure levels. Aliquots of 1 ml of each solution in the dilution series were transferred to the filter paper lined glass vials, allowing the hexane solvent to evaporate within 10 min. The filter paper was moistened with 1 ml of distilled water prior to the worms being placed into the vials.

Ten worms of average weight of 1.6 g of the species *E. veneta* were selected and exposed at each dose level. The levels of TFMA are given in table 1, along with the apparent physical effect on the worms. The earthworms were exposed to TFMA on the filter paper for 3 days. At the end of the study, surviving worms were snap-frozen in liquid nitrogen and stored at –20 °C until sample preparation for NMR analyses was carried out. The coelomic fluids expressed as a consequence of severe chemical irritation (at the lethal exposure levels) were combined with the individual host worms and immediately frozen (–20 °C). The worms were then homogenized directly into a physiological 1 ml Ringer solution (Goven *et al.* 1993) at pH 7.3, using an Ultra Turrax homogenizer (Model T25). The homogenates were subsequently ultra-centrifuged (MSE, Micro Centaur, 13 000 rpm for 5 min) and 500 µl of the

Biomarkers Downloaded from informahealthcare.com by Changhua Christian Hospital on 11/18/12
For personal use only.

RIGHTSLINK

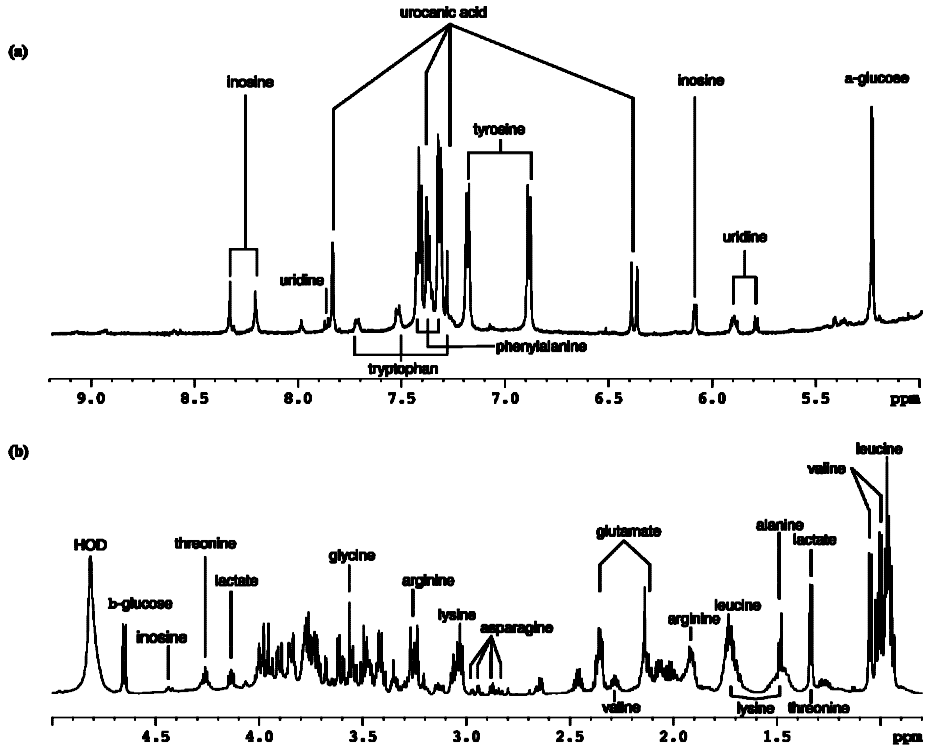

Figure 1. Typical ^{1}H NMR spectrum of control *Eisenia veneta* with the major metabolites assigned.

supernatant of each sample were directly transferred into NMR tubes. Subsequently, 100 µl aliquots of D_2O containing the internal reference standard, TSP (sodium 3-trimethlsilylproprionate-2,2,3,3-d_4), were added to the samples to provide a field-frequency lock for NMR spectroscopic measurements. Five worms from each of the dose groups were available for analysis by ^{1}H NMR.

^{1}H NMR spectroscopy of tissue extracts

^{1}H NMR spectra of the extracted earthworm homogenates were acquired on a Bruker AMX600 spectrometer operating at 600.13 MHz. Single pulse ^{1}H NMR spectra were obtained over a spectral width of 12 ppm (7201.56 Hz) utilizing a 9.14 µs pulse width (90° pulse angle) and stored as 64K data points. Typically, 128 transients were collected, with a relaxation delay of 1 s, an acquisition time of 4.44 s (resulting in a total pulse recycle time of 5.44 s). Solvent (residual water) suppression was achieved by the application of the NOESYPRESAT pulse sequence (Bruker 1996), which involves irradiation of the water frequency during the relaxation delay and the mixing time (100 ms). Spectra were transformed into 64K data points, manually phased and baseline corrected. For all spectra the internal chemical shift reference TSP singlet signal was set at $\delta = 0.0$.

Data reduction and analysis

The NMR spectra were data reduced using the AMIX ® v.2 program (Bruker 1996), whereby selected spectral regions were divided into segments of designated size, e.g. 0.04 ppm. The area of the signal under each segment was then integrated and these values used in the proceeding pattern recognition studies. The residual water signal (δ 4.9–4.7) was excluded from the analysis. The correlation principal component analysis (PCA) and single-link hierarchical cluster analysis (HCA) were performed using the JMP v.3.2 ® program. The mean, standard deviation, Pearson's correlation coefficient (r) and complete enumeration cluster significance analysis (CSA) were calculated in Excel97® using the formula and sort commands.

Results

A typical ^{1}H NMR spectrum of control *E. veneta* is shown in figure 1, with a selection of the known endogenous metabolites labelled. The scaling of the

Biomarkers Downloaded from informahealthcare.com by Changhua Christian Hospital on 11/18/12
For personal use only.

RIGHTSLINK

Table 2. Chemical shifts and multiplicity of endogenous metabolites found in Ringer extracts of *Eisenia veneta*.

Metabolite	Chemical shift (δ)	Multiplicity
Acetate	1.92	s
Acetone	2.14	s
Alanine	1.48, 3.79	d, m
Arginine	1.66, 1.73, 1.92, 3.25, 3.77	m, m, m, t, t
Asparagine	2.86, 2.96, 4.00	dd, dd, dd
Aspartate	2.65, 2.84, 3.85	dd, dd, dd
Betaine	3.36, 3.91	s, s
Citrate	2.65, 2.79	d, d (AB)
Formate	8.46	s
Fumarate	6.52	s
α-glucose	3.41, 3.54, 3.70, 3.77, 3.83, 3.83, 5.23	t, dd, t, t, dd, dddd, d
β-glucose	3.24, 3.40, 3.47, 3.49, 3.72, 3.89, 4.65	dd, t, dddd, t, t, dd, d
Glutamate	2.10, 2.36, 3.77	m, dt, t
Glycine	3.57	s
Histidine	3.14, 3.25, 3.99, 7.18, 7.98	dd, dd, dd, s, s
Inosine	3.85, 3.92, 4.28, 4.44, 6.10, 8.24, 8.34	dd, dd, q, t, d, s, s
Isoleucine	0.94, 1.01, 1.26, 1.48, 1.98, 3.68	t, d, m, m, m, d
Lactate	1.34, 4.15	d, q
Leucine	0.96, 1.71, 3.73	t, m, t
Lysine	1.48, 1.73, 1.91, 3.03, 3.76	m, qu, m, t, t
N-methyl-nicotinamide	4.48, 8.23, 8.95, 9.10, 9.30	s, t, d, d, s(br)
Orotic acid	6.20	s
Phenylalanine	3.13, 3.28, 4.00, 7.33, 7.39, 7.43	dd, dd, dd, d, t, t
Succinate	2.42	s
Threonine	1.33, 3.59, 4.26	d, d, dq
Tryptophan	3.31, 3.49, 4.06, 7.21, 7.29, 7.33, 7.55, 7.74	dd, dd, dd, t, t, s, d, d
Tyrosine	3.06, 3.20, 3.94, 6.91, 7.20	dd, dd, dd, d, d
Uridine	3.81, 3.92, 4.14, 4.24, 4.36, 5.90, 5.92, 7.87	dd, dd, q, t, t, s, d, d
Urocanic acid	6.40, 7.31, 7.41, 7.89	d, d, s, s
Valine	0.99, 1.04, 2.28, 3.62	d, d, m, d

d, doublet; dd, doublet of doublets; dt, doublet of triplets; m, unresolved multiplet; q, quartet; qu, quintet; s, singlet; t, triplet; (br) broad signal; (AB) non-degenerate CH_2.

aromatic region, figure 1(a), was several times larger than the aliphatic region, figure 1(b). In the aromatic region there were few metabolites, yet there was still overlap of the signals from protons of urocanic acid, typtophan and phenylaniline. The region above 8.5 ppm showed no appreciable metabolite signals. Other signals observed from endogenous metabolites include inosine, uridine and at lower chemical shift the anomeric proton of α-glucose. A full list of the metabolites identified and their NMR spectral data are given in table 2.

The residual water signal (HOD) was found around 5 ppm, with the anomeric proton signal of β-glucose at 4.65 ppm (figure 1(b)). Between 3.0 and 4.2 ppm there were a plethora of signals from the rest of the protons of the two glucose forms, and from endogenous amino acids. The overlap of signals in this region made assignment of signals from the 1-D ^{1}H NMR spectrum alone difficult. Various amino acid signals were seen throughout the aliphatic region frequency range, including those of alanine, arginine, asparagine, glycine, leucine, lysine, threonine and valine.

PR analysis of the full ^{1}H NMR spectrum

The initial PR analysis was performed on the whole spectrum (δ 10.0–0.2) excluding the water signal using the standard 0.04 ppm (24 Hz) segment width

Biomarkers Downloaded from informahealthcare.com by Changhua Christian Hospital on 11/18/12
For personal use only.

RIGHTSLINK

Biomarkers Downloaded from informahealthcare.com by Changhua Christian Hospital on 11/18/12
For personal use only.

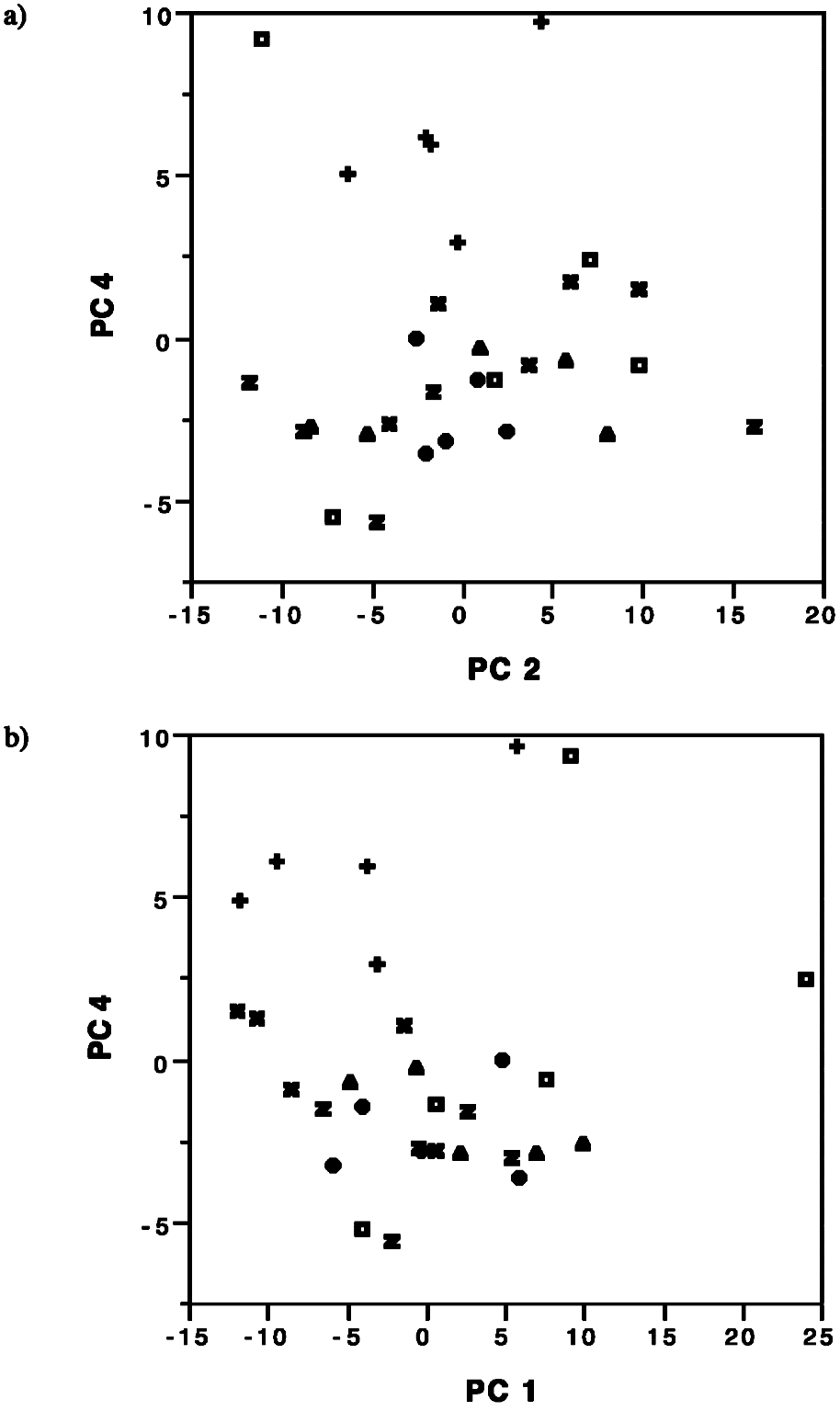

Figure 2. PCA of the entire spectrum (a) for PC2 vs PC4 and (b) with 'noise reduction' for PC1 vs PC4. (+) Dose 1; (×) dose 2; (¶) dose 3; (z) dose 4; (v) dose 5; (m) control.

RIGHTSLINK

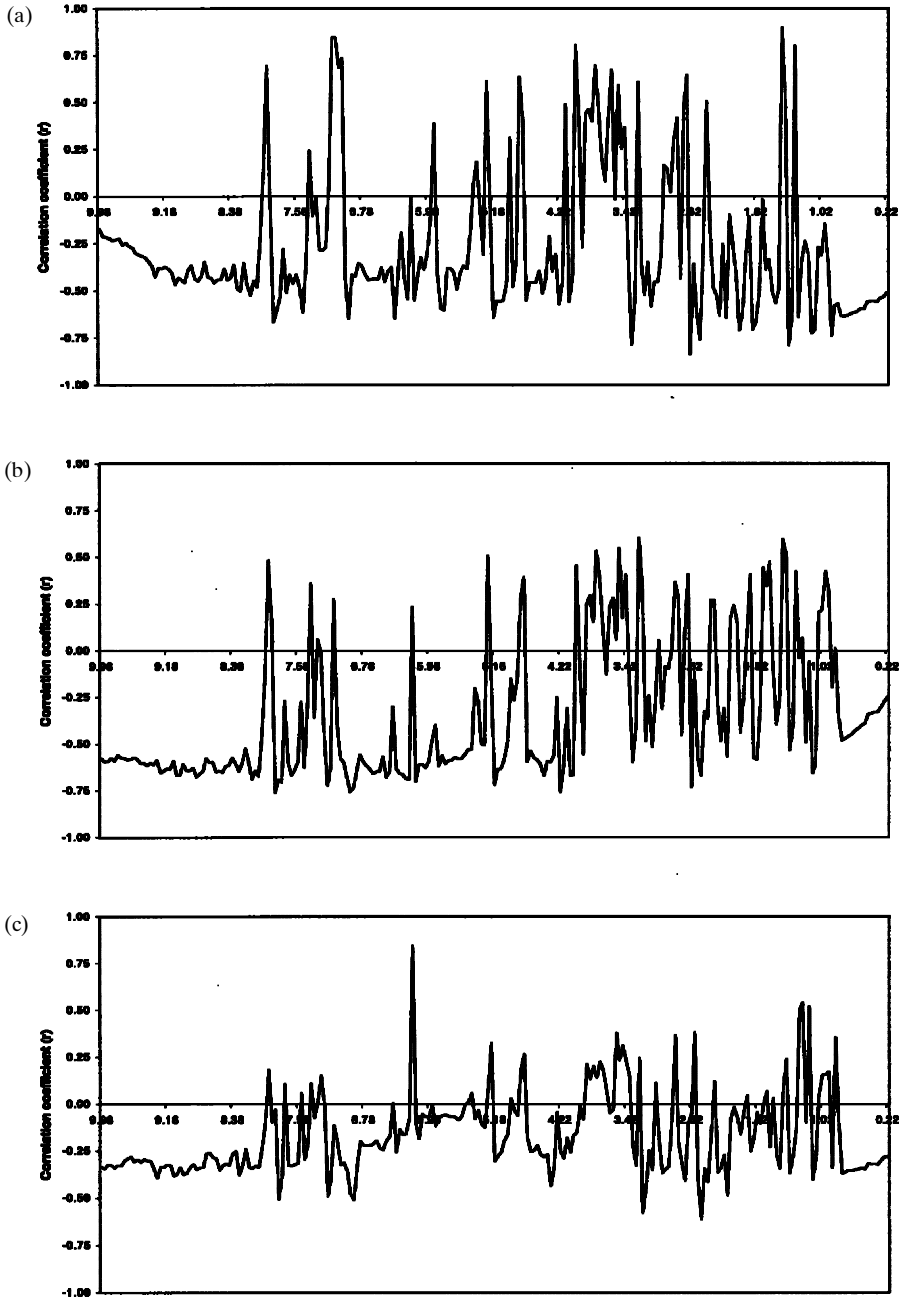

Figure 3. For legend see opposite.

Biomarkers Downloaded from informahealthcare.com by Changhua Christian Hospital on 11/18/12
For personal use only.

RIGHTSLINK

Biomarkers Downloaded from informahealthcare.com by Changhua Christian Hospital on 11/18/12
For personal use only.

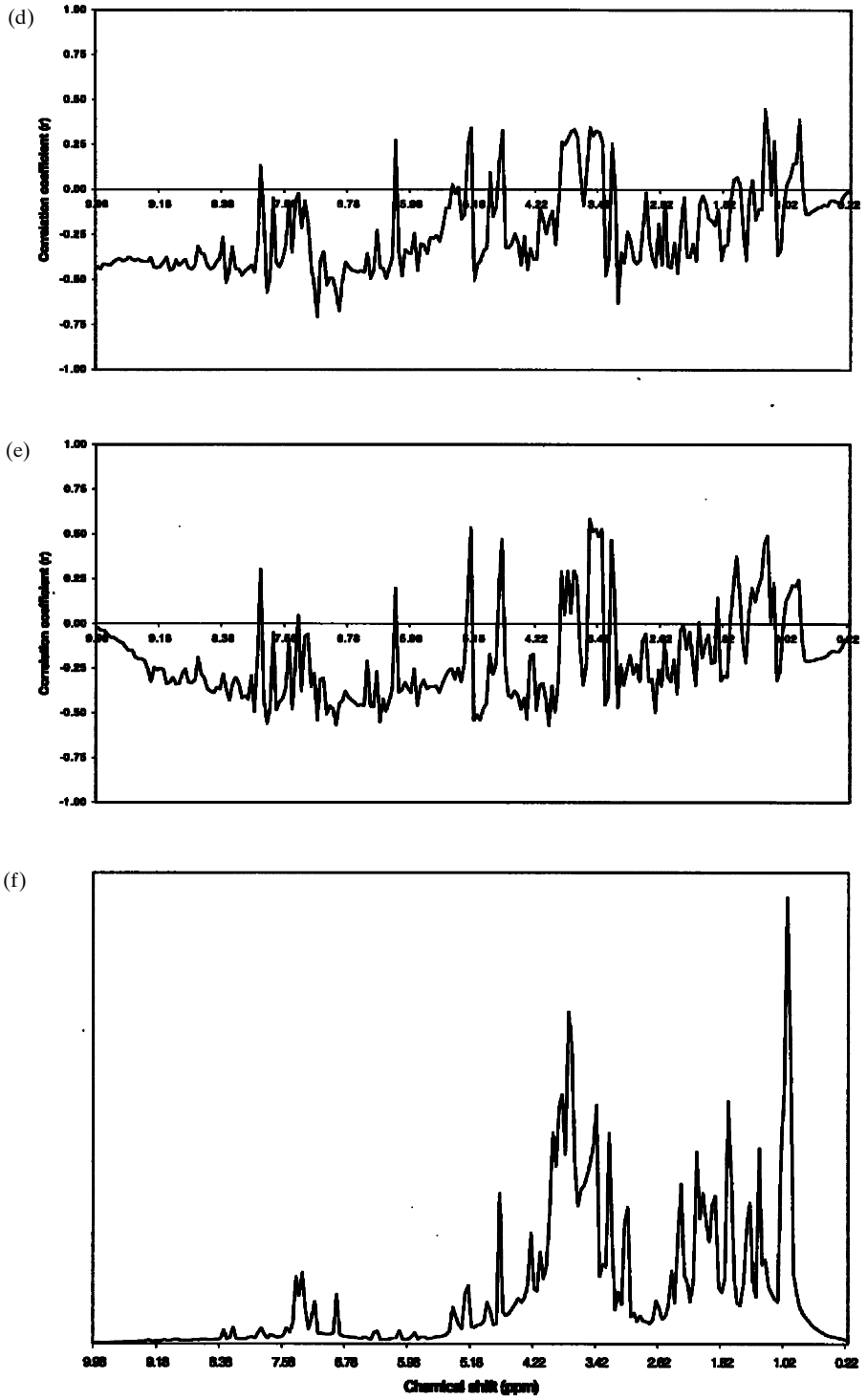

Figure 3. Plots of Pearson's correlation coefficient for dose class versus control for (a) dose 1, (b) dose 2, (c) dose 3, (d) dose 4, (e) dose 5, and the (f) average control group data reduced full spectrum.

RIGHTSLINK

(Gibb *et al.* 1997a) which resulted in 241 segments for analysis. The PCA for the first two PC (principal components) which contained 59.8%, 41.6% and 18.2% respectively, of the overall variance showed no clustering of the samples for any of the dose levels. The same was true of the PC1 vs PC3 and PC2 vs PC3. The first obvious classification of any of the dose levels appeared in the plots of PC2 vs PC4 and PC3 vs PC4. In figure 2(a) it can be seen that the highest dosed group (**+,** dose 1) was separated from the rest of the samples mostly by PC4 (6.4% of the variance). There was also a suggestion that the second highest dose level (×, dose 2) was slightly separated with three of the five samples with large PC4 values. However, the first three PCs (75.3% of the overall variance) contained a significant amount of information that was not contributing towards any biological (dose) classification. One method of removing some of this unwanted variation in the spectrum was to exclude the 'noise' from the spectrum. The 'mean noise' was calculated for each sample from the first 15 segments of the spectrum (δ 10.00–9.60) which was known to contain no detectable metabolite signals in any sample (Gibb *et al.* 1997a). The noise contribution was subtracted from all the segments, and then any segments with less than 10 times the 'noise level' was removed to leave 184 spectral segments for analysis. The PCA was altered from the uncorrected one, although there was no improvement in the clustering of points according to their dose in the most significant PC. The best classification was now given by PC1 vs PC4, figure 2(b), where four of the dose 2 data points grouped near the separated highest dose level.

It was of interest to determine the biochemical changes that separated dose 1 and some of dose 2 from the other samples. This was accomplished by comparing each dose group separately against the control data using the segments for the uncorrected full spectrum. A class variable was introduced which for instance, the five samples of dose 1 were given a value of one and the five control samples a value of zero. For these 10 samples each segment was compared with the class variable and the correlation coefficient (r) obtained. The values for all the segments were then visually displayed against the chemical shift in figure 3 for each dose group. The larger the absolute value of correlation coefficient the greater the dose classification of the segment. A positive coefficient indicated an increase in the segment area in the dosed samples, a negative value a decrease.

It can be seen from figure 3(a) the positive correlation coefficients for dose 1 were generally greater than those found for any other dose group (figure 3(b–e)). This highlighted why this dose separated from the others in the PCA. It was noteworthy that dose 2 showed the next highest correlations, with dose 3–dose 5 similar to the control. From the correlation coefficient-shift plots key individual metabolites of biochemical response can be selected. For instance, for dose 1 (figure 3(a)) alanine (β-Me at δ 1.48) and the dosed TFMA (H2, H4, H5, and H6 at δ 7.18–6.98) both had large positive coefficients. Similarly, for dose 3 (figure 3(c)) the only high positive correlation was for the alkene proton of orotic acid (δ 6.18). A list of the significant metabolites is given in table 3, and these will be discussed later. The average control spectrum after data reduction is shown in figure 3(f).

It was also intriguing to examine the value of the coefficients (r) at the extreme ends of the correlation coefficient-shift plots that contain only noise (cf. figure 3(f)). For these regions (10–8.4 ppm and 0.7–0.2 ppm) there was often a reasonable negative correlation, e.g. ca –0.6 in figure 3(b) for dose 2. This was presumably due to variation in the noise level or baseline for these groups compared with the control, despite baseline correction on the processed spectra. This could indicate

Biomarkers Downloaded from informahealthcare.com by Changhua Christian Hospital on 11/18/12
For personal use only.

RIGHTSLINK

Table 3. Changes in endogenous metabolites in response to TFMA toxicity in *Eisenia veneta*.

Segment (δ)	Significance Dose 1	Significance Dose 2	Metabolite	Proton(s)
Full spectrum at 0.04 ppm segments:				
7.92–7.96	*	–	Unknown	
7.00–7.16	***	–	TFMA‡	H2, H4, H5, H6
5.24–5.28	*	–	α-Glucose	H1
4.68–4.72	*	–		
4.00–4.04	***	–		
3.76–3.80	**	–		
3.56–3.60	*	–		
3.24–3.28	*	*	See below	
2.64–2.68	*	–		
1.48–1.52	***	*		
1.32–1.36	***	–		
Aliphatic region at 0.02 ppm segments:				
4.66–4.68	**	–	β-Glucose	H1
4.00–4.02	**	–	Overlapped α-CH amino acids (1)	
3.78–3.80	***	*	Overlapped sugars and amino acids (2)	
3.56–3.58	***	–	Glycine	CH_2
3.48–3.50	*	–	Overlapped sugars	
3.24–3.26	–	*	Overlapped sugars	
2.94–2.96	*	–	Asparagine	CH_2
2.88–2.90	*	–	Asparagine	CH_2
2.78–2.80	**	–	Citrate	CH_2
2.66–2.68	***	–	Citrate	CH_2
2.40–2.42	**	–	Succinate	CH_2
1.48–1.50	***	*	Alanine	β-CH_3
1.34–1.36	***	–	Lactate and/or threonine	β-CH_3 CH_3

(1) includes asparagine α-CH; (2) includes alanine α-CH.
*** $r > 0.8$; ** $0.8 > r > 0.7$; * $0.7 > r > 0.6$; ‡ dosed compound.

Biomarkers Downloaded from informahealthcare.com by Changhua Christian Hospital on 11/18/12
For personal use only.

significant differences in the concentration of the samples for dose 1 and dose 2 compared with the control samples, perhaps due to the release of coelomic fluid and evaporation of the most volatile components. In the data reduction stage the normalization factor would be different between these groups, and for noise that was not a function of the sample concentration different integrals obtained. Indeed this may suggest a reason why there was little dose classification in the first three PCs.

PR analysis of the aliphatic region of the ^1H NMR spectrum

Another method of removing some of the unwanted variation in the spectra was to consider only the aliphatic region of the spectrum that contained the majority of the signals, and perhaps most of the toxin-induced changes. The exclusion of the noise level was unnecessary since nearly all of the segments in this region (δ 4.7–0.7) were many hundreds times the noise level. Secondly, this excluded those peaks in the aromatic region that were most solvent sensitive, e.g. histidines ring proton at δ 7.71 that moved ca 0.1 ppm between samples. This was a source of variation not related to the change in metabolite levels. Further, this also excluded some small resonances due to NH protons at δ 8.98–9.30 with solvent variable line width, which appeared and disappeared into the noise apparently at random. Finally, the appearance of the dosed compound, TFMA in the highest dosed group

RIGHTSLINK

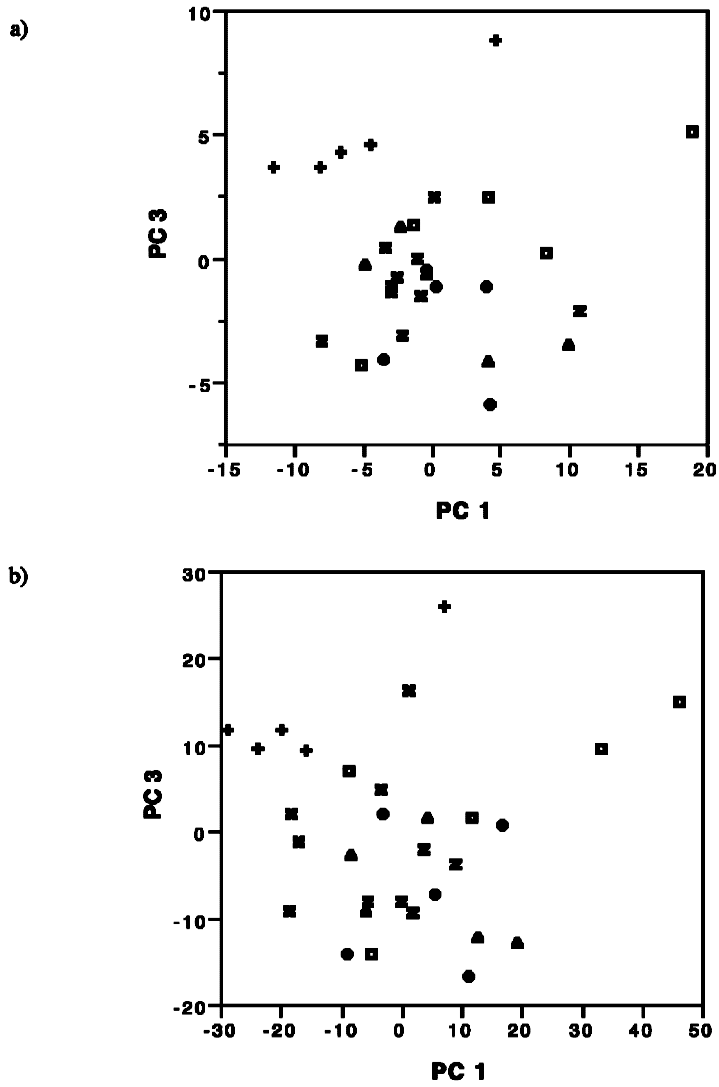

Figure 4. PCA of the aliphatic region (a) for PC1 vs PC3 at 0.04 ppm segment width, and (b) for PC1 vs PC3 at 0.005 ppm segment width. (+) Dose 1; (×) dose 2; (¶) dose 3; (z) dose 4; (v) dose 5; (m) control.

Biomarkers Downloaded from informahealthcare.com by Changhua Christian Hospital on 11/18/12
For personal use only.

suggested a 0.2 ppm portion of the aromatic region should be excluded from the analysis. For subsequent dosed compounds other aromatic regions may need to be excluded, suggesting the exclusion of the most of the aromatic region in comparative studies.

It was seen that PC1 and PC2 (cumulatively containing 64.3% of the overall variance) still showed no dose classification, although in figure 4(a), the PC1–PC3 plot, there was clear separation in PC3 for the highest dose level. The segments that contribute to the separation of the highest dose level have moved from PC4 to PC3 suggesting some reduction in the unwanted variation in the spectra. Although PC3 (containing 11.0% of the overall variance) appeared to be the major contributor there was also some contribution to the separation from PC1.

RIGHTSLINK

Biomarkers Downloaded from informahealthcare.com by Changhua Christian Hospital on 11/18/12
For personal use only.

To obtain better definition and some further separation the size of the segment areas were reduced for the spectral range δ 4.7–0.7. This was particularly important in the aliphatic region where the signals from many metabolites overlap. If the segment width was too large no change may be recorded when one metabolite increased and another equally decreased. From the initial segment width of 0.04 ppm (24 Hz) incremental reductions in the width by a factor of two were performed to a minimum of 0.005 ppm (3 Hz). As the segment width was reduced the five data points for the second highest group level, along with one of the control data points emerged from the rest to form a region between the highest dose level. In figure 4(b) at 0.005 ppm segment width the two highest dose levels, apart from one control data point now formed distinct clusters away from the other samples. Further dose 4 (z) appeared as a tight cluster in the centre of the PC1–PC3 plane. The other dose levels, dose 3 and dose 5, were approximately centred about the same region as dose 4 but with much greater variance. The control group showed the greatest variance of all the groups with two data points at extreme PC1 values, two data points around dose 3–dose 5 region and one data point overlapping into the dose 2 region. It was thus apparent that the separation of the lower dose groups was more variance related, than with a distinctly different centre.

To verify the apparent clustering in one of the lowest dose groups, CSA was carried out on the first three PCs with the segment width at 0.005 ppm. CSA was originally devised for the classification of active and non-active groups (McFarland and Dans 1986), although the situation here of control and dosed was analogous. The limitation of CSA of only comparing two classes of biological response at one time (McFarland and Dans 1987) was accommodated by comparing each dose group with control separately. The results of the CSA for each dose group are given in table 4, where the probability represented the likelihood that the cluster would have arisen purely by chance.

It can be seen immediately that dose 4 clustered well in the PC1–PC3 plane ($p = 0.008$) and this was due to the optimal clustering in PC3 ($p = 0.004$). In contrast the clustering of dose 3 and dose 5 was poor in the PC1–PC3 plane, and this was observed by eye in figure 4(b). The highest dose showed a reasonable clustering ($p = 0.040$) although dose 2 was outside the 95% confidence limit. These two groups are however separated by their position in the PC1–PC3 plane and not necessarily their clustering. CSA thus provides a means of pattern verification of clustering potential.

Further, the CSA shows that dose 5 was optimally clustered in the PC2–PC3 plane ($p = 0.004$), while dose 3 clustered well in PC3 alone ($p = 0.020$). However, it should be remembered that visually not only the position of the five control and the five dosed samples, but also the position of all the dose groups influence human perception.

Mean PC plots and PCA of mean spectra

The PC1–PC3 plot in figure 4(b) is represented in figure 5 with the same axes but with mean dose positions and standard deviation ellipses. Each point represents an average of five samples forming the centre of the ellipse, and the two principal ellipse axes were calculated from the standard deviation of the five samples in PC1 and PC3. This enabled the visualization of the dose–response function. The control group was found at positive PC1 and PC3 values, with the lowest dosage

RIGHTSLINK

Table 4. CSA probability of each dose group clustering by chance compared with the control group for the first three PC.

Dose	PC1	PC2	PC3	
1	0.0794	0.0357	0.2659	
2	0.0873	0.2381	0.4603	
3	0.1587	0.2381	0.0198	
4	0.0357	0.6905	0.0040	
5	0.1230	0.0159	0.1389	
Dose	PC1–PC2	PC1–PC3	PC2–PC3	PC1–PC2–PC3
1	0.0516	0.0397	0.0595	0.0278
2	0.0635	0.0595	0.2103	0.0595
3	0.1190	0.1071	0.0794	0.0714
4	0.1984	0.0079	0.5555	0.1349
5	0.0119	0.1032	0.0040	0.0159

Biomarkers Downloaded from informahealthcare.com by Changhua Christian Hospital on 11/18/12
For personal use only.

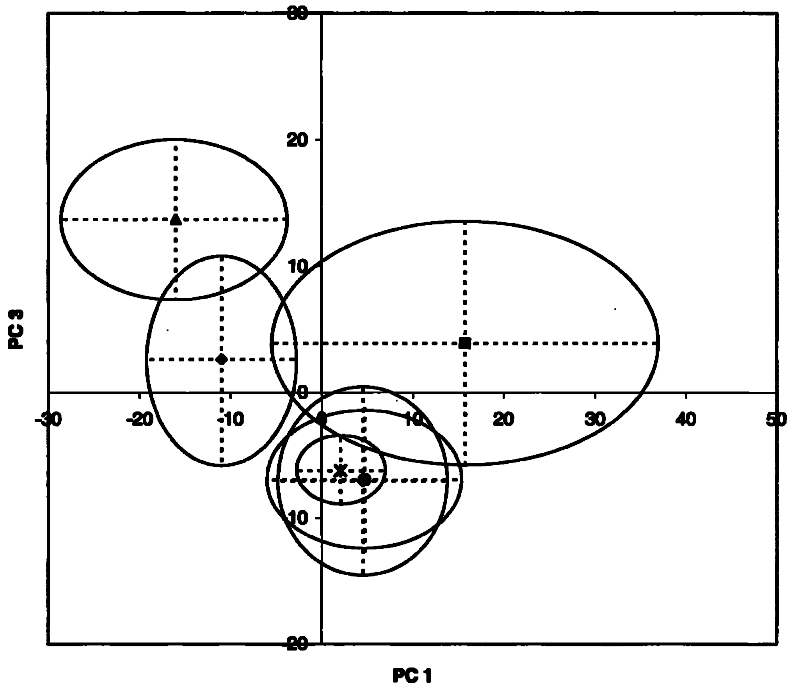

Figure 5. Mean dose position ± standard deviation ellipse for each dose group in PC1–PC3 plot of the aliphatic region at 0.005 ppm segment width. (¶) Dose 1; (◆) dose 2; (V) dose 3; (×) dose 4; (+), dose 5; (m) control.

levels (dose 3–dose 5) at negative PC3 values. The response function then passed to negative PC1 and PC3 values with increasing dose level (dose 2 and dose 1); this formed an inverted 'tick'. This could be used to identify the comparative dose of a TFMA-contaminated worm, remembering that the variation in the lowest dose levels allowed no definitive classification, and the variation in the control group was large. Figure 5 also allowed the visualization of the smaller variation in dose 4 group as noted previously by the CSA.

RIGHTSLINK

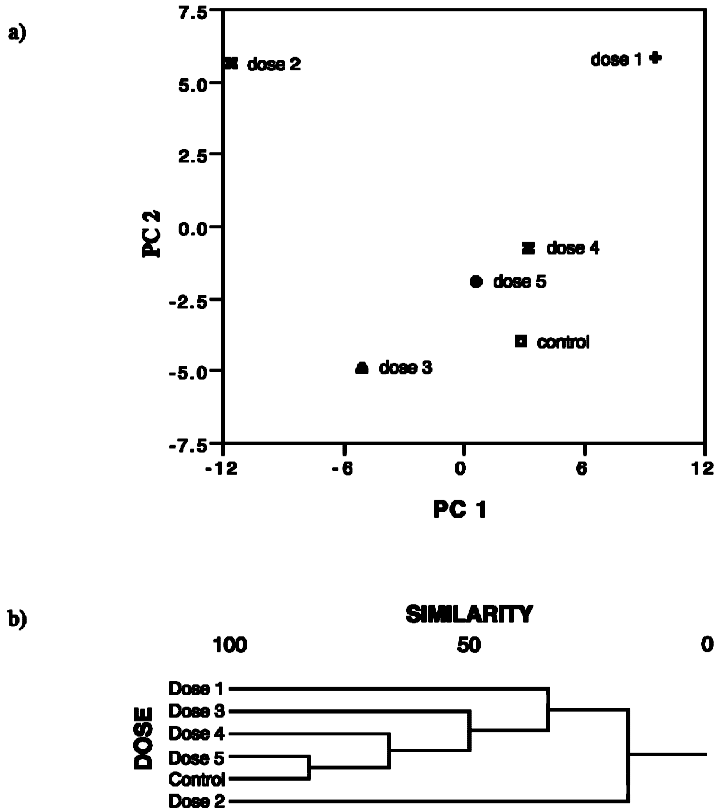

Figure 6. (a) PCA and (b) HCA of the average spectra at 0.04 ppm segment width for the aliphatic region.

In previous NMR-PR studies the PC maps calculated from mean NMR integral values have been used to display time-related trajectories of toxicity, e.g. Beckwith-Hall *et al.* (1998). This method may also be applied to display the dose–response function. Hence the PC plot of the mean spectra for each dose group is given in figure 6(a), this time for the full spectrum at 0.04 ppm segment width. This clearly showed dose 1 and dose 2 separated at extreme PC1 and PC2 values, despite the poorer separation seen for the PCA of the individual samples. The lower dose groups (dose 3–dose 5) clustered near the control average spectra point. The dose–response function was no longer obvious. This may be expected from the change in the PCs as figure 6(a) was based upon only six data points, while the mean PCA in figure 5 was based upon 30 samples.

The similarity of the lower dosage groups was shown in figure 6(b) in the HCA. Dose 5 was the most similar to the control followed by dose 4, then dose 3 with the two highest dose levels the least similar.

Changes in endogenous metabolite levels

The changes in the metabolite profile displayed visually in figure 3(a–e) are summarized in table 3 for the most significant descriptors. The correlation coefficient-shift plots showed a large negative baseline effect for dose 1 and dose 2, and although there were large negative correlations suggesting some reduction of

Biomarkers Downloaded from informahealthcare.com by Changhua Christian Hospital on 11/18/12
For personal use only.

RIGHTSLINK

certain metabolites, their real significance was difficult to judge. Instead the large positive correlations were chosen at a low threshold of 0.6 for possibly significant (*), 0.7 for significant (**), and 0.8 for very significant (***).

For the whole spectrum at 0.04 ppm segments there were 15 regions of interest, with eight of these signals to high field of the water signal ($\delta < 4.7$). If the aliphatic region was considered in more detail at 0.02 ppm segments there are now 13 segments of significance, suggesting that better definition of the metabolite profile was useful. Assignment of the metabolites was by visual inspection of the NMR spectra for the selected regions and comparison with known chemical shifts and couplings (table 1). The signals from the dosed TFMA were found by comparison with the standard and the rest from literature assignments (Gibb *et al.* 1997b).

In the aromatic region there was one metabolite which, due to poor signal to noise, was unidentified. At lower chemical shift there were increasing levels of the glucose forms clearly seen for the H1 signals, and presumably those significant regions containing overlapping sugar signals are due to the other glucose protons. Increases in the levels of amino acids, namely glycine, asparagine, alanine and perhaps threonine, were also significant. Changes in the levels of citrate and succinate, both part of the citric acid cycle, were also found. The largest change was noted for the signal from the β-methyl group in alanine, indicating this as the best marker of TFMA toxicity.

Biomarkers Downloaded from informahealthcare.com by Changhua Christian Hospital on 11/18/12
For personal use only.

Discussion

A preliminary appraisal of the metabonomic approach in invertebrate toxicity studies

Clearly the ^{1}H NMR spectra of earthworm extracts are responsive to toxic stimuli caused by the exposure to 3TFMA *in vivo*. Detailed analyses of the NMR data (see below) show that clear cut combination biomarker responses to the toxic effects of 3TFMA are present. Given that the ^{1}H NMR spectra of extracts take only a few minutes to perform and are associated with a very low recurrent cost there is clearly potential for the use of this technology in ecotoxicological screening in the future. Moreover, as NMR spectroscopy is a molecular structure elucidation tool the technique shows not only as a mere detector of toxic effect, but provides direct structural information on potential biomarkers. Furthermore, for some metabolites the biomarker responses may have direct mechanistic significance, which may also be of toxicological value.

Detailed analysis of NMR spectral data

The investigation of the effect of noise, spectral width and segment width of the NMR spectra of *E. veneta* as displayed using PCA of the integrated segments have shown varying effects on the dose classification. The most significant improvement in the classification was probably the consideration of the aliphatic region alone, where the separation of the highest dose group moved from the PC1–PC4 to the PC1–PC3 plane. However, the reduction of the segment width in this area containing many overlapped signals from different metabolites enabled the separation of the second highest dose group as well. Further, dose 4 appeared to show significantly less variability than the other low dose levels. Finally, the mean PCA ellipses allowed easier visualization of the relative position of the groups within the plot, and the dose–response function.

RIGHTSLINK

The improvement of the classification in the PC plots coincided with the increase in significant descriptors or biomarkers, as demonstrated in table 3. This helped to confirm the PCA was describing real changes in metabolite levels, and not just solvent shifts of signals or contributions from the baseline. A more detailed examination of the eigenvectors showed a remarkable similarity between the significant contributors to PC3 for the aliphatic region with those found to be significant in the correlation coefficient-shift plots. For example, from the 13 aliphatic regions selected in table 3, 10 of these regions contributed highly (> 0.11) to PC3 of the relevant PCA, and two of the remaining three regions to PC1. Of course, the PCA contains important contributions from other regions not selected by the correlation coefficient analysis, so there is probably a more optimal linear separation possible using discriminant analysis; this will await consideration of further toxicants.

The PCA appeared to suggest the two highest dose levels are distinct from the three lowest doses, and these in turn from the control group. While there were distinct markers of toxicity for dose 1 and dose 2, only orotic acid was notable for dose 3, with the next highest change for δ 1.24–1.28 ($r = 0.540$). For dose 4 and dose 5 the correlations were even lower, yet it seems the sum of the small differences for dose 3–dose 5 across the aliphatic region contributed together to separate them from the control group in the PC plot. Hence, PCA as a multiple linear combination of variables was superior to simply selecting biomarker for classifying the lowest dose groups.

It may be possible to alter the experimental conditions to obtain better classification of the dose–response of earthworms away from the standard 72-h filter paper test. For instance, Beckwith-Hall *et al.* (1998) noted for hepatotoxicity to rat using the NMR-PR approach that the maximum non-permanent biochemical effect occurred at the 24–32 h period. While, a similar analysis has not been performed for earthworms the maximum reversible toxicological effect (non-lethal) may be within the first 2 days of the experiment before excretion of the toxin or metabolites. Alternatively, permanent changes in the metabolic profile may result from exposure to low levels of the compound over weeks, months or even generations. These effects and their time-scale are dependent upon the nature of the toxicant used. Despite these provisos with the experimental arrangement it is still possible to obtain some useful toxicological information from the basic LC_{50} filter paper test.

Final conclusion

Overall, it has been demonstrated here that ^{1}H NMR-based metabonomic analysis affords a useful approach to the investigation of biochemical toxic effects in environmentally relevant invertebrate species, and a novel means of obtaining biomarker information. Future work will concentrate on the toxicity of a variety of halogenated aromatic compounds to common earthworm species using this methodology. This should help to develop a common set of biomarkers towards this class of industrial pollutants.

Acknowledgements

We thank the NERC Environmental Diagnostics Programme (Grant GST/02/1591) for financial support (M.A.W. and E.L).

Biomarkers Downloaded from informahealthcare.com by Changhua Christian Hospital on 11/18/12
For personal use only.

RIGHTSLINK

References

ANTHONY, M. L., SWEATMAN, B. C., BEDDELL, C. R., LINDON, J. C. and NICHOLSON, J. K. 1994, Pattern recognition classification of the site of nephrotoxicity based on metabolic data derived from proton nuclear magnetic resonance spectra of urine. *Molecular Pharmacology*, **46**, 199–211.

BECKWITH-HALL, B. M., NICHOLSON, J. K., NICHOLLS, A. W., FOXALL, P. J. D., LINDON, J. C., CONNOR, S. C., ABDI, M., CONNELLY, J. and HOLMES, E. 1998, Nuclear magnetic resonance spectroscopic and principal components analysis investigations into biochemical effects of three model hepatotoxins. *Chemical Research in Toxicology*, **11**, 269–72.

BRUKER ANALYTISCHE MESSTECHNIK GMBH, Silberstreiben, Germany, 1996.

GARTLAND, K. P. R., BEDDELL, C. R., LINDON, J. C. and NICHOLSON, J. K. 1991, Application of pattern-recognition methods to the analysis and classification of toxicological data derived from proton nuclear magnetic resonance spectroscopy of uridine. *Molecular Pharmacology*, **39**, 629–642.

GIBB, J. O. T., SVENDSEN, C., WEEKS, J. M. and NICHOLSON, J. K. 1997a, ^{1}H NMR spectroscopic investigations of tissue metabolite biomarker response to Cu(II) exposure in terrestrial invertebrates: identification of free histidine as a novel biomarker of exposure to copper in earthworms. *Biomarkers*, **2**, 295–302.

GIBB, J. O. T., HOLMES, E., NICHOLSON, J. K. and WEEKS, J. M. 1997b, Proton NMR spectroscopic studies on tissue extracts of invertebrate species with pollution indicator potential. *Comparative Biochemistry and Physiology*, **118B**, 587–598.

GOVEN, A. J., EYAMBE, G. S., FITZPATRICK, L. C., VENABLES, B. J. and COOPER, E. L. 1993, Cellular biomarkers for measuring toxicity of xenobiotics–effects of polychlorinated-biphenyls on earthworm *Lumbricus terrestrius* celomocytes. *Environmental Toxicology and Chemistry,* **12**, 863–870.

HOLMES, E., NICHOLSON, J. K., NICHOLLS, A. W., LINDON, J. C., CONNOR, S. C., POLLEY, S. and CONNELLY, J. 1998, The identification of novel biomarkers of renal toxicity using automatic data reduction techniques and PCA of proton NMR spectra of urine. *Chemometrics and Intelligent Laboratory Systems*, **44**, 245–255.

HOLMES, E., LINDON, J. C. and NICHOLSON, J. K. 'Metabonomics': Understanding the metabolic responses of living systems to pathophysiological stimuli via multivariate statistical analysis of biological NMR spectroscopic data. *Xenobiotica*, **29**, 1181–1189.

JMP version 3.2. SAS Institute Inc., SAS Campus Drive, Cary, NC 27513.

LIVINGSTONE, D. 1995, *Data Analysis for Chemists* (Oxford: Oxford University Press).

MCFARLAND, J. W. and GANS, D. J. 1986, On the significance of clusters in graphical display of structure–activity data. *Journal of Medicinal Chemistry*, **29**, 505–514.

MCFARLAND, J. W. and GANS, D. J. 1987, Cluster significance analysis contrasted with three other quantitative structure–activity relationship methods. *Journal of Medicinal Chemistry*, **30**, 46–49.

NICHOLSON, J. K. and WILSON, I. D. 1989, High resolution proton magnetic resonance spectroscopy of biological fluids. *Progress in NMR Spectroscopy*, **21**, 449–501.

NICHOLSON, J. K., TIMBRELL, J. and SADLER, P. J. 1985, Proton NMR spectra of uridine as indicators of renal damage–mercury induced nephrotoxicity in rats. *Molecular Pharmacology*, **27**, 644–657.

OECD guideline for testing of chemicals, No.207, adopted April 4 1984, 'Earthworm, *acute toxicity tests*, Organisation for Economic Co-operation and Development (OECD)'.

PAYAPEREZ, A. B. and MANNONE, P. 1997, Toxicity of chloroanilines to the earthworm '*Eisenia foetida*' by soil tests. *Fresenius Environmental Bulletin,* **6**, 410–417.

PAYAPEREZ, A. B., MANNONE, P. and SKEJOANDRESEN, H. 1995, Toxicity of chloroanilines to the earthworm *Eisenia-foetida*. *Fresenius Environmental Bulletin,* **4**, 47–52.

VAN GESTEL, C. A. M. 1991, *Earthworms in Ecotoxicology* (Utrecht, The Netherlands: University of Utrecht).

VAN GESTEL, C. A. M. and MA, W. C. 1990, An approach to quantitative structure–activity-relationships (QSARs) in earthworm toxicity studies. *Chemosphere*, **21**, 1023–1033.

VAN GESTEL, C. A. M. and MA, W. C. 1993, Development of QSARs in terrestrial ecotoxicology–earthworm toxicity and soil sorption of chlorophenols, chlorobenzenes and chloroanilines. *Water, Sea and Air Pollution*, **69**, 265–276.

VAN GESTEL, C. A. M., MA, W. C. and SMIT, C. E. 1991, Development of QSARs in terrestrial ecotoxicology–earthworm toxicity and soil sorption of chlorophenols, chlorobenzenes and dichloroaniline. *Science of the Total Environment*, **109/110**, 589–604.

Biomarkers Downloaded from informahealthcare.com by Changhua Christian Hospital on 11/18/12
For personal use only.

RIGHTSLINK